

Cosmic Dispersion Measure from Gamma-Ray Burst Afterglows: Probing the Reionization History and the Burst Environment

Kunihito Ioka

Department of Earth and Space Science, Osaka University, Toyonaka 560-0043, Japan

ioka@vega.ess.sci.osaka-u.ac.jp

ABSTRACT

We show a possible way to measure the column density of free electrons along the light path, the so-called Dispersion Measure (DM), from the early [$\sim 415(\nu/1 \text{ GHz})^{-2}(\text{DM}/10^5 \text{ pc cm}^{-3}) \text{ s}$] radio afterglows of the gamma-ray bursts. We find that the proposed Square Kilometer Array can detect bright radio afterglows around the time $\sim 10^3(\nu/160 \text{ MHz})^{-2} \text{ s}$ to measure the intergalactic DM ($\gtrsim 6000 \text{ pc cm}^{-3}$ at redshift $z > 6$) up to $z \sim 30$, from which we can determine the reionization history of the universe and identify the missing warm-hot baryons. At low z , DM in the host galaxy may reach $\sim 10^5 \text{ pc cm}^{-3}$ depending on the burst environment, which may be probed by the current detectors. Free-free absorption and diffractive scattering may also affect the radio emission in a high density.

Subject headings: gamma rays: bursts — intergalactic medium — ISM: general — plasmas — radio continuum: ISM

1. Introduction and summary

Many observations support a massive star origin for long-duration Gamma-Ray Bursts (GRBs). Although the nature of the central engine that accelerates the GRB jets remains unknown, the afterglows are successfully fitted by the synchrotron shock model for probing the jet properties and burst environment (e.g., Mészáros 2002).

On the other hand, GRBs may be useful for probing high redshift z (e.g., Miralda-Escudé 1998; Barkana & Loeb 2003; Inoue, Yamazaki, & Nakamura 2003). Their high luminosities make them detectable even at $z \sim 100$ (Lamb & Reichart 2000), while the X-ray and infrared afterglows are observable up to $z \sim 30$ (Ciardi & Loeb 2000; Gou et al. 2003) and provide their z through the Ly α break (Lamb & Reichart 2000) or Fe lines

(Mészáros & Rees 2003), in contrast to galaxies or quasars which are likely dimmer at higher z . About 25% of all GRBs detected by the upcoming *Swift* satellite, due for launch in 2003 December, are expected to be at $z > 5$ (Bromm & Loeb 2002). High z GRBs may have already been detected by BATSE based on the empirical luminosity indicators (Fenimore & Ramirez-Ruiz 2000; Norris, Marani, & Bonnell 2000; Murakami et al. 2003; Yonetoku et al. 2003), for which some theoretical explanations exist (e.g., Ioka & Nakamura 2001a). The first generation stars could be very massive (Abel, Bryan, & Norman 2002; Bromm, Coppi, & Larson 2002; Omukai & Palla 2003), so that they may end as brighter GRBs (Mészáros & Rees 2003).

In this Letter, we show that free electrons along the light path cause distortion in the spectrum and light curve of an early radio afterglow, from which we can measure the column density of the free electrons, the so-called Dispersion Measure (DM). This is because, in a plasma with an electron density n_e , an electromagnetic wave with frequency $\nu (\gg \nu_p)$ is delayed relative to in a vacuum by a time

$$\Delta t \simeq \int \frac{dl}{c} \frac{\nu_p^2}{2\nu^2} = 415 \left(\frac{\nu}{1 \text{ GHz}} \right)^{-2} \left(\frac{\text{DM}}{10^5 \text{ pc cm}^{-3}} \right) \text{ s}, \quad (1)$$

where $\nu_p = (n_e e^2 / \pi m_e)^{1/2} = 8.98 \times 10^3 n_e^{1/2}$ Hz is the plasma frequency and $\text{DM} = \int n_e dl$ (Rybicki & Lightman 1979). DMs of pulsars are well studied by using the arrival time of pulses at two or more frequencies (Taylor, Manchester, & Lyne 1993). Our method to measure DMs of GRBs is somewhat different since we do not assume simultaneously emitted pulses but the afterglow model. We can determine DM only from a single-band light curve around the time $t \sim \Delta t$ (see §3). The former method was suggested by Ginzburg (1973) and Palmer (1993) before the discovery of the afterglows.

At $z > 6$, DM_{IGP} due to the intergalactic plasma (IGP) will be $\gtrsim 6000 \text{ pc cm}^{-3}$ [correspondingly $\Delta t \gtrsim 10^3 (\nu/160 \text{ MHz})^{-2} \text{ s}$], and probably dominate DM_{G} due to the Galactic plasma and DM_{host} due to the plasma in the host galaxy (see §2). DM_{IGP} as a function of z varies depending on the reionization history of the universe since recombined electrons provide no DM (see §4). Thus, from DMs of GRBs at various z and directions, we can determine the reionization history, and possibly even map the topology of the ionized bubbles. The reionization history is now actively investigated but remains unclear (Miralda-Escudé 2003). The analysis of the Ly α spectra in the highest z quasars suggests that the reionization ends at $z \sim 6$ (Fan et al. 2002), while the WMAP polarization data imply a much higher reionization redshift $z \sim 17 \pm 5$ (Kogut et al. 2003; Spergel et al. 2003). In §4, we show that the proposed Square Kilometer Array (SKA) can detect bright afterglows at $t \sim \Delta t$ to measure DM_{IGP} up to $z \sim 30$. In addition, observations of DM_{IGP} could also identify the ‘missing’ baryons that have not been detected at $z \lesssim 1$ (see §2).

At low z , DM_{host} in the host galaxy may reach $\sim 10^5$ pc cm $^{-3}$ and dominate DM_G and DM_{IGP} depending on the as-yet-unknown burst environment (see §2). Since we may target low z GRBs, even current detectors could detect afterglows at $t \sim \Delta t$ to constrain DM_{host} and the GRB environment. Throughout we adopt a Λ CDM cosmology with $(\Omega_m, \Omega_\Lambda, \Omega_b, h, \sigma_8) = (0.27, 0.73, 0.044, 0.71, 0.84)$ (Spergel et al. 2003).

2. Expected Dispersion Measure (DM)

Galactic DM_G : The distribution of free electrons in our Galaxy is relatively well known from observations of pulsar DMs, and we can estimate DM_G as a function of the Galactic latitude and longitude (Taylor & Cordes 1993). DM_G has its maximum (minimum) in the direction parallel (perpendicular) to the Galactic plane, ranging from

$$DM_G^{\text{min}} \sim 30 \text{ pc cm}^{-3} \quad (2)$$

to $DM_G^{\text{max}} \sim 10^3 \text{ pc cm}^{-3}$ (Taylor et al. 1993; Nordgren, Cordes, & Terzian 1992).

Intergalactic DM_{IGP} : We first estimate DM_{IGP} assuming that all baryons are fully ionized and homogeneously distributed, so that the free electron density evolves as $n_e = (3H_0^2\Omega_b/8\pi Gm_p)(1+z)^3$. Then the observed dispersion delay at an observed frequency ν for a source at z is given by $\Delta t = \int_0^z dz |dt/dz|(1+z)\nu_p^2/2[\nu(1+z)]^2 = 415(\nu/1 \text{ GHz})^{-2} (DM_{\text{IGP}}/10^5 \text{ pc cm}^{-3}) \text{ s}$, where $|dt/dz|^{-1} = (1+z)H_0[\Omega_m(1+z)^3 + \Omega_\Lambda]^{1/2}$ and

$$DM_{\text{IGP}} = \frac{3cH_0\Omega_b}{8\pi Gm_p} \int_0^z \frac{(1+z)dz}{[\Omega_m(1+z)^3 + \Omega_\Lambda]^{1/2}}. \quad (3)$$

From Figure 1, $DM_{\text{IGP}} > DM_G^{\text{min}}$ at $z > 0.03$.

More than half of all baryons have not been detected at $z \lesssim 1$ (Fukugita, Hogan, & Peebles 1998). Most of such 'missing' baryons may reside in a warm-hot IGP, which is difficult to observe because of its high temperature (10^5 - 10^7 K) and low density (moderate overdensity 10-40) (Cen & Ostriker 1999; Davé et al. 2001). If so, an appreciable fraction of DM_{IGP} ($\gtrsim 500 \text{ pc cm}^{-3}$) comes from the missing baryons at $0 \leq z < 1$ (see Figure 1). Thus observations of DM_{IGP} could be a direct detection of the missing baryons.

DM_{host} in host galaxy: A host galaxy has been found in most GRBs (Bloom, Kulkarni, & Djorgovski 2002). If the host galaxies are similar to ours, they have $DM_{\text{host}} \sim DM_G$. At high z , the maximum and minimum DM_{host} may evolve as $\sim DM_G^{\text{max}}(M/10^{12}M_\odot)(1+z)^3$ and $\sim DM_G^{\text{min}}(M/10^{12}M_\odot)^{1/3}(1+z)^2$, respectively, for a host galaxy with the halo mass M based on the hierarchical galaxy formation (Ciardi & Loeb 2000). Even at low z , DM_{host} may be

high if GRBs arise from the star forming regions, as expected in GRBs resulting from massive stellar collapses. The hydrogen column density is as high as 10^{22} - 10^{23} cm^{-2} in giant molecular clouds (Galama & Wijers 2001), and the prompt and afterglow emission with energy E_{ion} erg can ionize the ambient density n_{host} cm^{-3} out to a distance of $d \sim 160 n_{\text{host}}^{-1/3} E_{\text{ion},52}^{1/3}$ pc (Perna & Loeb 1998), where the convention $Q = 10^x Q_x$ is used. Thus all the ambient hydrogen may be ionized depending on its density. In this case, $\text{DM}_{\text{host}} \sim 10^3$ - 10^5 pc cm^{-3} , which may be time-dependent (Perna & Loeb 1998). A high DM is also expected in the ‘supranova’ model (Vietri & Stella 1998), in which a supernova (SN) occurs weeks before the GRB. A SN remnant shell with mass M g and velocity v cm s^{-1} reaches at $R \sim 10^{16} v_9 t_7$ cm in t s, which provides $\text{DM}_{\text{host}} \sim M/4\pi R^2 m_p \sim 1.5 \times 10^5 v_9^{-2} t_7^{-2} M_{33}$ pc cm^{-3} . The shell may be clumpy for normal GRBs and afterglows to be detected.

Anyway, the maximum DM_{host} allowed by the present observations is about the inverse of the Thomson cross section σ_T ,

$$\text{DM}_{\text{host}}^{\text{max}} \sim \sigma_T^{-1} \sim 4.87 \times 10^5 \text{ pc cm}^{-3}, \quad (4)$$

for GRBs and afterglows to be observed without scattering. Correspondingly, $\Delta t_{\text{host}} \sim 2022(\nu_{\text{host}}/1 \text{ GHz})^{-2}$ s from equation (1). At high z , the observed dispersion delay and frequency are $\Delta t = (1+z)\Delta t_{\text{host}}$ and $\nu = \nu_{\text{host}}/(1+z)$, respectively. Thus it is convenient to use $\text{DM}_{\text{host}}(z) = \text{DM}_{\text{host}}/(1+z)$ to compare it with DM_{G} and DM_{IGP} . From Figure 1, $\text{DM}_{\text{host}}(z)$ declines with increasing z while DM_{IGP} grows. Therefore, GRBs at high (low) z are suitable for measuring DM_{IGP} (DM_{host}).

3. DM from dispersed afterglows

We now study the effects of the plasma dispersion on the afterglow emission. For illustrative purposes we fix DM demanding the observed dispersion delay of $\Delta t = 10^3(\nu/1 \text{ GHz})^{-2}$ s in this section. We consider the most simple but standard afterglow model (Sari, Piran, & Narayan 1998), which reproduces the observations very well. Extensions to other models, such as the wind environment model (e.g., Chevalier & Li 2000) and so on (see §5), are straightforward.

The afterglow spectrum for the forward shock is well approximated by four power law segments with breaks at cooling frequency ν_c , typical frequency ν_m and self-absorption frequency ν_a . In the fast cooling case, $(\nu_a <) \nu_c < \nu_m$, the spectrum is $F_\nu \propto \nu^2, \nu^{1/3}, \nu^{-1/2}, \nu^{-p/2}$ from low to high frequencies, and has a maximum flux $F_{\nu,\text{max}}$ at $\nu = \nu_c$. In the slow cooling, $(\nu_a <) \nu_m < \nu_c$, it is $F_\nu \propto \nu^2, \nu^{1/3}, \nu^{-(p-1)/2}, \nu^{-p/2}$, and peaks at $\nu = \nu_m$. Assuming an

adiabatic shock, we have the observed break frequencies and maximum flux as

$$\begin{aligned}
 \nu_c &= 2.5 \times 10^{13} \epsilon_B^{-3/2} E_{52}^{-1/2} n^{-1} t_3^{-1/2} (1+z)^{-1/2} \text{ Hz}, \\
 \nu_m &= 4.2 \times 10^{18} \epsilon_B^{1/2} \epsilon_e^2 g^2 E_{52}^{1/2} t_3^{-3/2} (1+z)^{1/2} \text{ Hz}, \\
 F_{\nu, \text{max}} &= 1.1 \times 10^5 \epsilon_B^{1/2} E_{52} n^{1/2} D_{28}^{-2} (1+z) \mu\text{Jy},
 \end{aligned} \tag{5}$$

where E erg is the isotropic equivalent shock energy, $n \text{ cm}^{-3}$ is the constant surrounding density, ϵ_e (ϵ_B) is the electron (magnetic) energy fraction, t s is the observer time, D cm is the luminosity distance and $g = (p - 2)/(p - 1)$. At $\nu < \nu_a$, synchrotron self-absorption limits the flux below the blackbody emission with the electron temperature (e.g., Sari & Piran 1999; Kobayashi & Sari 2000). This is given by

$$F_{\nu, \text{BB}} = 2\pi\nu^2 \gamma \gamma_e m_e (R_{\perp}/D)^2 (1+z), \tag{6}$$

where ν is the observed frequency, γ is the Lorentz factor of the shocked fluid, $R_{\perp} = 4\gamma ct$ is the observed size of the afterglow and γ_e is the typical Lorentz factor of the electrons emitting at ν . A reverse shock is also formed, but its temperature is lower because of its higher density, making its emission dimmer at $\nu < \nu_a$.

A dispersed afterglow is readily obtained by replacing t with $t - \Delta t$ in the above expressions. From Figure 2, we can see that the spectrum has a cutoff at $\nu \sim 1(t/\Delta t_{\text{GHz}})^{-1/2}$ GHz when the dispersion delay is $\Delta t = \Delta t_{\text{GHz}}(\nu/1 \text{ GHz})^{-2}$ where we are using $\Delta t_{\text{GHz}} = 10^3$ s. The light curve deviates from the power law at $t \sim \Delta t$. Measurements of these features yield Δt and hence DM with equation (1). In practice, DM may be treated as an additional fitting parameter. Only a single-band light curve will suffice to measure DM, but a multi-band observation will be useful to exclude other interpretations, such as variable light curves seen in GRB 021004 and GRB 030329 (e.g., Uemura et al. 2003) and microlensing (Loeb & Perna 1998; Ioka & Nakamura 2001b), by using the frequency dependence $\Delta t \propto \nu^{-2}$.

4. Prospects for probing the reionization

DM_{IGP} varies depending on the reionization history, as shown by the dashed lines in Figure 1. DM_{IGP} is a constant $\sim 6000 \text{ pc cm}^{-3}$ at $z > z_{\text{reion}}$ if a sudden reionization occurred at $z_{\text{reion}} = 6$, while $\text{DM}_{\text{IGP}} \sim 12000 \text{ pc cm}^{-3}$ if $z_{\text{reion}} = 17$. We also show the case when the reionization occurred twice at $z_{\text{reion}} = 6, 20$ with a full recombination at $z = 15$ (Cen 2003a,b; Wyithe & Loeb 2003). Contrary to the Ly α absorption (Inoue et al. 2003), DM can determine the reionization history even if the neutral fraction is $\gtrsim 10^{-5}$ during the first reionized era.

Can we measure DMs of high z GRBs ? We should start a radio follow-up within $\sim \Delta t \sim 972 (\nu/160 \text{ MHz})^{-2} (\text{DM}/6000 \text{ pc cm}^{-3}) \text{ s}$, since DM distorts the light curve at $t \sim \Delta t$ (see Figure 2). This may be possible since *Swift* will send a 1-4 arcmin GRB position to the ground within $\sim 1 \text{ min}$ (see <http://swift.gsfc.nasa.gov/>). The dispersion delay Δt is longer at lower frequencies, but the flux decays as $F_\nu \propto \nu^2$ at $\nu < \nu_a$. Here we adopt $\nu = 160 \text{ MHz}$ assuming a response time of $t \sim 10^3 \text{ s}$. In Figure 3, the afterglow flux at $\nu = 160 \text{ MHz}$ and $t = 10^3 \text{ s}$ is plotted as a function of z . For the typical parameters, $E = 10^{52} \text{ erg}$, $n = 1 \text{ cm}^{-3}$, $\epsilon_e = 0.1$, $\epsilon_B = 0.01$ and $p = 2.2$, the flux is too dim to be detected even by SKA, whose rms sensitivity is $\sim 0.3 (\Delta\nu/80 \text{ MHz})^{-1/2} \tau_3^{-1/2} \mu\text{Jy}$ for a band width $\Delta\nu \sim 0.5\nu$, an integration time $\tau = 10^3 \text{ s}$ and $A_{\text{eff}}/T_{\text{sys}} = 2 \times 10^8 \text{ cm}^2 \text{ K}^{-1}$ (see <http://www.astron.nl/skai/science/>). However some GRBs have larger energy $E \sim 10^{54} \text{ erg}$ and lower density $n \sim 10^{-2} \text{ cm}^{-3}$ (Panaitescu & Kumar 2002). From Figure 3, such GRBs can be detected as $\sim 7\sigma$ events even at $z = 15$ by SKA, and dominate the host galaxy emission even if $\text{SFR} \sim 100 M_\odot \text{ yr}^{-1}$ at $z \gtrsim 8$. Note that the density around the first stars could be $10^{-2} \lesssim n \lesssim 1 \text{ cm}^{-3}$ because of strong radiation pressure from the central massive star (Whalen, Abel, & Norman 2003; Gou et al. 2003). On the contrary, the density could evolve as $n \propto (1+z)^4$ for a fixed host galaxy mass based on the hierarchical galaxy formation (Ciardi & Loeb 2000). If $n \sim (1+z)^4 \text{ cm}^{-3}$, we will never detect radio afterglows at high z (see Figure 3).

5. Discussions

Free-free absorption (FF) may be important when the ambient density $n_{\text{host}} \text{ cm}^{-3}$ is high. The host galaxy is optically thick to FF at $\nu \lesssim 2(\text{DM}_{\text{host}}/10^5 \text{ pc cm}^{-3})^{1/2} T_4^{-3/4} n_{\text{host},3}^{1/2} (1+z)^{-1} \text{ GHz}$ where T is the plasma temperature in K (Rybicki & Lightman 1979). In this case we cannot measure DM but can probe the burst environment. We may neglect FF in IGP at $\nu \gtrsim 1.6 h^{3/2} \Omega_{b,-2} \Omega_{m,-1}^{-1/4} T_4^{-3/4} (1+z)^{5/4} \text{ kHz}$ where $z \gg 1$ (Rees 1978).

Density fluctuations cause a dispersion in DM_{IGP} . For example, if the average number of intervening gas clumps with a DM of Σ is N , the dispersion $\langle (\Delta\text{DM})^2 \rangle$ is $\sim N\Sigma^2$. We may roughly estimate $\langle (\Delta\text{DM})^2 \rangle$ using the Press-Schechter theory. Kitayama & Suto (1996) derived the comoving number density of halos that form with mass $M \sim M + dM$ at time $z_f \sim z_f + dz_f$ and are observed at z , $F(M, z_f; z) dM dz_f$. If the halo mass is $M \lesssim 10^{12} M_\odot$, the inside gas can cool to have a radius $r_d \sim 0.035 r_{\text{vir}}$ (e.g., Ciardi & Loeb 2000), otherwise $r_d \sim r_{\text{vir}}$, where $r_{\text{vir}}(M, z_f)$ is the virial radius of the halo. Then, DM of one halo is about $\Sigma(M, z_f; z) = M\Omega_b/2\pi r_d^2 m_p \Omega_m (1+z)$, and the dispersion of DM due to halos in a logarithmic mass interval is about $\langle [\Delta\text{DM}(M)]^2 \rangle \sim \int c dt \int dz_f \pi r_d^2 M F (1+z)^3 \Sigma^2$. We

calculate $\max\langle[\Delta\text{DM}(M)]^2\rangle$ and show it as the shaded region in Figure 1. It is about $\langle[\Delta\text{DM}(10^{12}M_\odot)]^2\rangle/\text{DM}^2 \sim (68\%)^2$ at $z = 1$. Unvirialized objects have less contributions since $\langle[\Delta\text{DM}(2 \times 10^{14}M_\odot)]^2\rangle/\text{DM}^2 \sim 8h^{-1} \text{ Mpc}/6.6 \text{ Gpc} \sim (4\%)^2$ at $z = 1$ for density fluctuations of radius $8h^{-1} \text{ Mpc}$.

At $\nu \lesssim \nu_s = 10 \text{ GHz}$, scintillation due to the Galactic plasma is in the strong scattering regime, so that diffractive and refractive scintillation take place (Goodman 1997; Walker 1998). Although the modulation index (rms fractional flux variation) is unity $m_s = 1$ for diffractive scintillation, the decorrelation bandwidth is very narrow $\Delta\nu_s/\nu = (\nu/\nu_s)^{17/5} \sim 4 \times 10^{-4}\nu_9^{17/5}$ at low frequencies. Then m_s will be reduced to $\sim \sqrt{\Delta\nu_s/\nu} \sim 2\nu_9^{17/10}\%$ for a broadband observation. For refractive scintillation, $m_s = (\nu/\nu_s)^{17/30} \sim 27\nu_9^{17/30}\%$. Thus Galactic scintillation may be quenched at $\nu \lesssim 1 \text{ GHz}$ with $\Delta\nu \sim \nu$. On the other hand, scattering in the host galaxy may cause temporal broadening of the early radio afterglows by a time $\sim 1/2\pi\Delta\nu_s \sim 10\nu_9^{-22/5}(\text{DM}_{\text{host}}/10^5 \text{ pc cm}^{-3})^{6/5}n_{\text{host},3}^{6/5}d_1(1+z)^{-17/5} \text{ s}$, if the scattering measure scales as $\propto ln_e^2$ (Goodman 1997), where d pc is the size of the ionized region.

We have neglected the inverse Compton cooling for the afterglow emission, which prolongs the fast cooling regime (Sari & Esin 2001). In the fast cooling regime, an additional power law segment $F_\nu \propto \nu^{11/8}$ may appear in the spectrum if the cooled electrons are layered (Granot, Piran, & Sari 2000). In addition, photons accumulating around the shock front may make the cooling ‘ultrafast’ (Ioka 2003). These are interesting future problems.

We are grateful to F. Takahara, J. Yokoyama, K. Omukai and M. Matsumiya for useful discussions. This work was supported in part by the Monbukagaku-sho Grant-in-Aid for Scientific Research, No. 00660.

REFERENCES

- Abel, T., Bryan, G. L., & Norman, M. L. 2002, *Science*, 295, 93
- Barkana, R., & Loeb, A. 2003, astro-ph/0305470
- Bloom, J. S., Kulkarni, S. R., & Djorgovski, S. G. 2002, *AJ*, 123, 1111
- Bromm, V., Coppi, P. S., & Larson, R. B. 2002, *ApJ*, 564, 23
- Bromm, V., & Loeb, A. 2002, *ApJ*, 575, 111
- Cen, R., & Ostriker, J. P. 1999, *ApJ*, 514, 1

- Cen, R. 2003a, *ApJ*, 591, 12
- Cen, R. 2003b, *ApJ*, 591, L5
- Chevalier, R. A., & Li, Z.-Y. 2000, *ApJ*, 536, 195
- Ciardi, B., & Loeb, A. 2000, *ApJ*, 540, 687
- Davé, R., et al. 2001, *ApJ*, 552, 473
- Fan, X., et al. 2002, *AJ*, 123, 1247
- Fenimore, E. E., & Ramirez-Ruiz, E. 2000, astro-ph/0004176
- Fukugita, M., Hogan, C. J., & Peebles, P. J. E. 1998, *ApJ*, 503, 518
- Galama, T. J., & Wijers, R. A. M. J. 2001, *ApJ*, 549, L209
- Ginzburg, V. L. 1973, *Nature*, 246, 415
- Gou, L. J., Mészáros, P., Abel, T., & Zhang, B. 2003, astro-ph/0307489
- Goodman, J. 1997, *NewA*, 2, 449
- Granot, J., Piran, T., & Sari, R. 2000, *ApJ*, 534, L163
- Inoue, A. K., Yamazaki, R., & Nakamura, T. 2003, astro-ph/0308206
- Ioka, K. 2003, *ApJ*, 583, 819
- Ioka, K., & Nakamura, T. 2001a, *ApJ*, 554, L163
- Ioka, K., & Nakamura, T. 2001b, *ApJ*, 561, 703
- Kitayama, T., & Suto, Y. 1996, *ApJ*, 469, 480
- Kobayashi, S., & Sari, R. 2000, *ApJ*, 542, 819
- Kogut, A., et al. 2003, *ApJ* in press (astro-ph/0302213)
- Lamb, D. Q., & Reichart, D. E. 2000, *ApJ*, 536, 1
- Loeb, A., & Perna, R. 1998, *ApJ*, 495, 597
- Mészáros, P. 2002, *ARA&A*, 40, 137
- Mészáros, P., & Rees, M. J. 2003, *ApJ*, 591, L91

- Miralda-Escudé, J. 1998, *ApJ*, 501, 15
- Miralda-Escudé, J. 2003, *Science*, 300, 1904
- Murakami, T., Yonetoku, D., Izawa, H., & Ioka, K. 2003, *PASJ*, 55, 2461
- Nordgren, T. E., Cordes, J. M., & Terzian, Y. 1992, *AJ*, 104, 1465
- Norris, J. P., Marani, G. F., & Bonnell, J. T. 2000, *ApJ*, 534, 248
- Oh, S. P. 2001, *ApJ*, 553, 499
- Omukai, K., & Palla, F. 2003, *ApJ*, 589, 677
- Palmer, D. M. 1993, *ApJ*, 417, L25
- Panaitescu, A. & Kumar, P. 2002, *ApJ*, 571, 779
- Perna, R., & Loeb, A. 1998, *ApJ*, 501, 467
- Rees, M. J. 1978, *Nature*, 275, 35
- Rybicki, G. B., & Lightman, A. P. 1979, *Radiative Processes in Astrophysics* (New York: Wiley Interscience)
- Sari, R., & Esin, A. A. 2001, *ApJ*, 548, 787
- Sari, R., & Piran, T. 1999b, *ApJ*, 517, L109
- Sari, R., Piran, T., & Narayan, R. 1998, *ApJ*, 497, L17
- Spergel, D. N. 2003, *ApJ* in press (astro-ph/0302209)
- Taylor, J. H., & Cordes, J. M. 1993, *ApJ*, 411, 674
- Taylor, J. H., Manchester, R. N., & Lyne, A. G. 1993, *ApJS*, 88, 529
- Uemura, M., et al. 2003, *Nature*, 423, 843
- Vietri, M., & Stella, L. 1998, *ApJ*, 507, L45
- Walker, M. A. 1998, *MNRAS*, 294, 307
- Whalen, D., Abel, T., & Norman, M. L. 2003, in preparation
- Wyithe, J. S. B., & Loeb, A. 2003, *ApJ*, 588, L69

Yonetoku, D., Murakami, T., Nakamura, T., Yamazaki, R., Inoue, A. K., & Ioka, K. 2003,
in preparation

Yun, M. S., & Carilli, C. L. 2002, ApJ, 568, 88

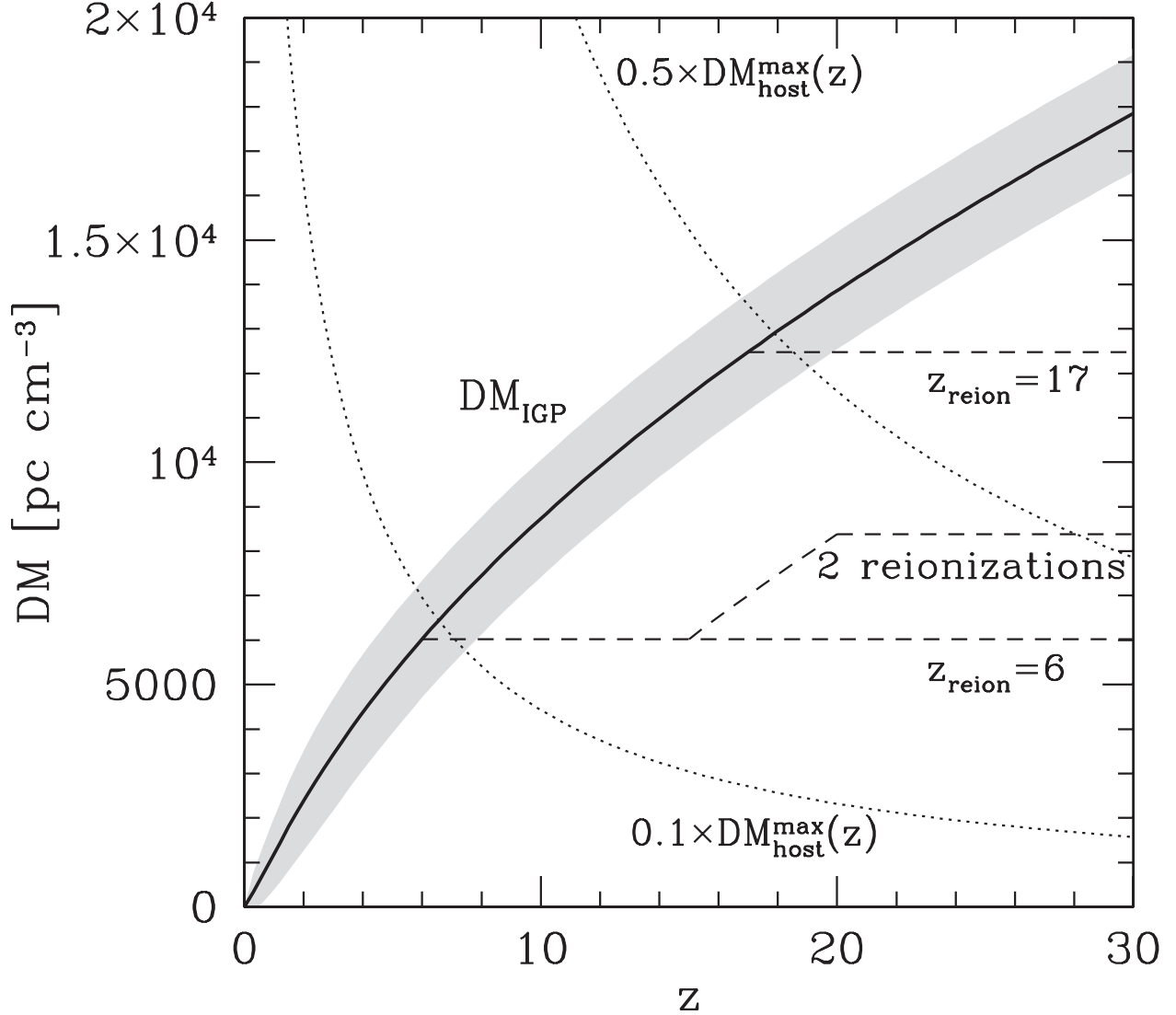


Fig. 1.— The Dispersion Measure (DM) due to the intergalactic plasma, DM_{IGP} , is plotted as a function of redshift z by the solid line. The dispersion of DM_{IGP} due to density fluctuations is shown by the shaded region. $0.5 \times DM_{\text{host}}^{\text{max}}(z)$ and $0.1 \times DM_{\text{host}}^{\text{max}}(z)$ are also shown by the dotted lines where $DM_{\text{host}}^{\text{max}}(z) = DM_{\text{host}}^{\text{max}}/(1+z)$ is the maximum DM due to the plasma in the host galaxy in equation (4). The dashed lines are DM_{IGP} for a sudden reionization at $z_{\text{reion}} = 6$, $z_{\text{reion}} = 17$ and the case when the reionization occurred twice at $z_{\text{reion}} = 6, 20$ with a full recombination at $z = 15$.

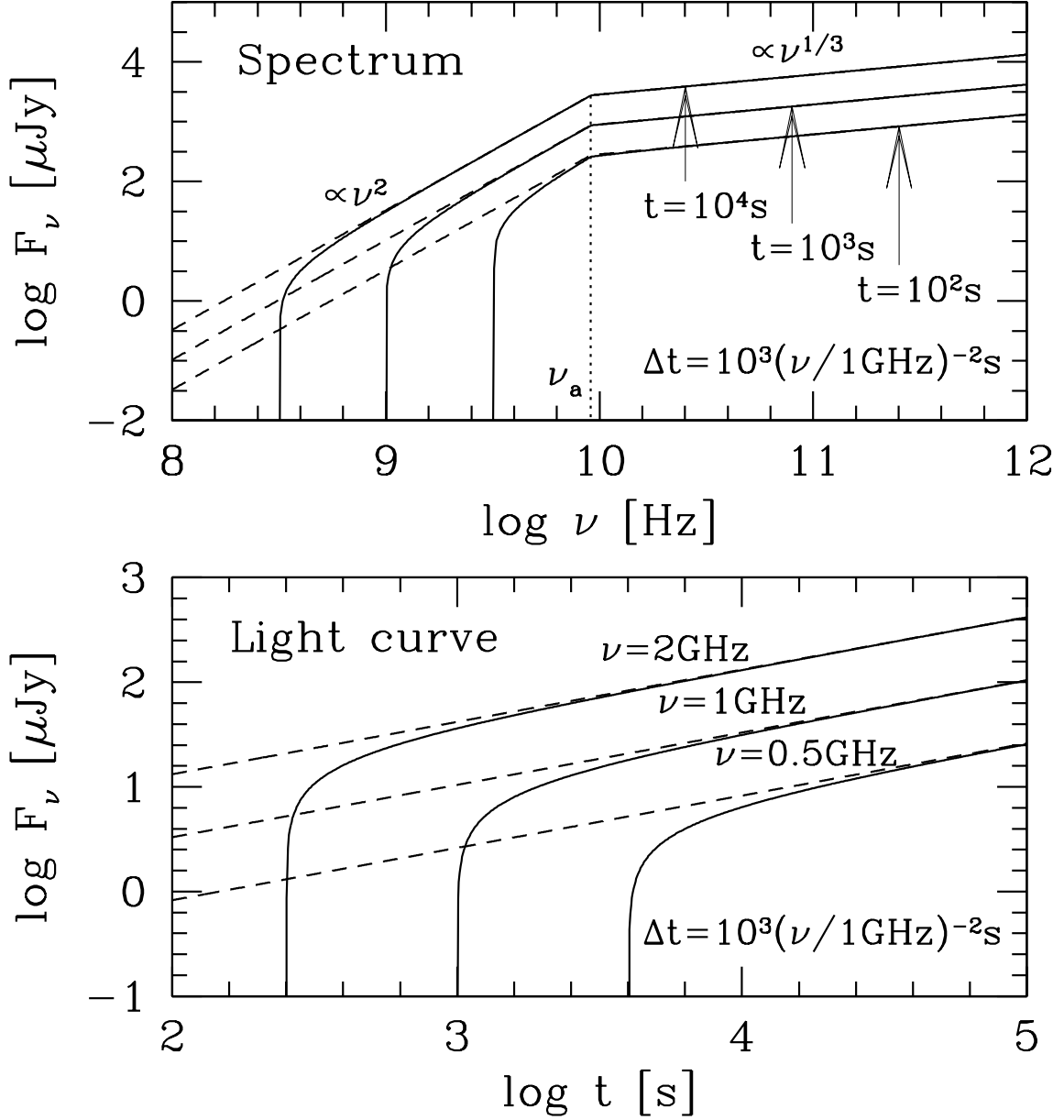


Fig. 2.— The spectra (*upper panel*) and light curves (*lower panel*) of afterglows are shown with and without the dispersion delay $\Delta t = 10^3(\nu/1\text{GHz})^{-2}\text{s}$ by the solid and dashed lines, respectively. We adopt $E = 10^{52}\text{erg}$, $n = 1\text{cm}^{-3}$, $\epsilon_e = 0.1$, $\epsilon_B = 0.01$, $p = 2.2$ and $z=0.5$.

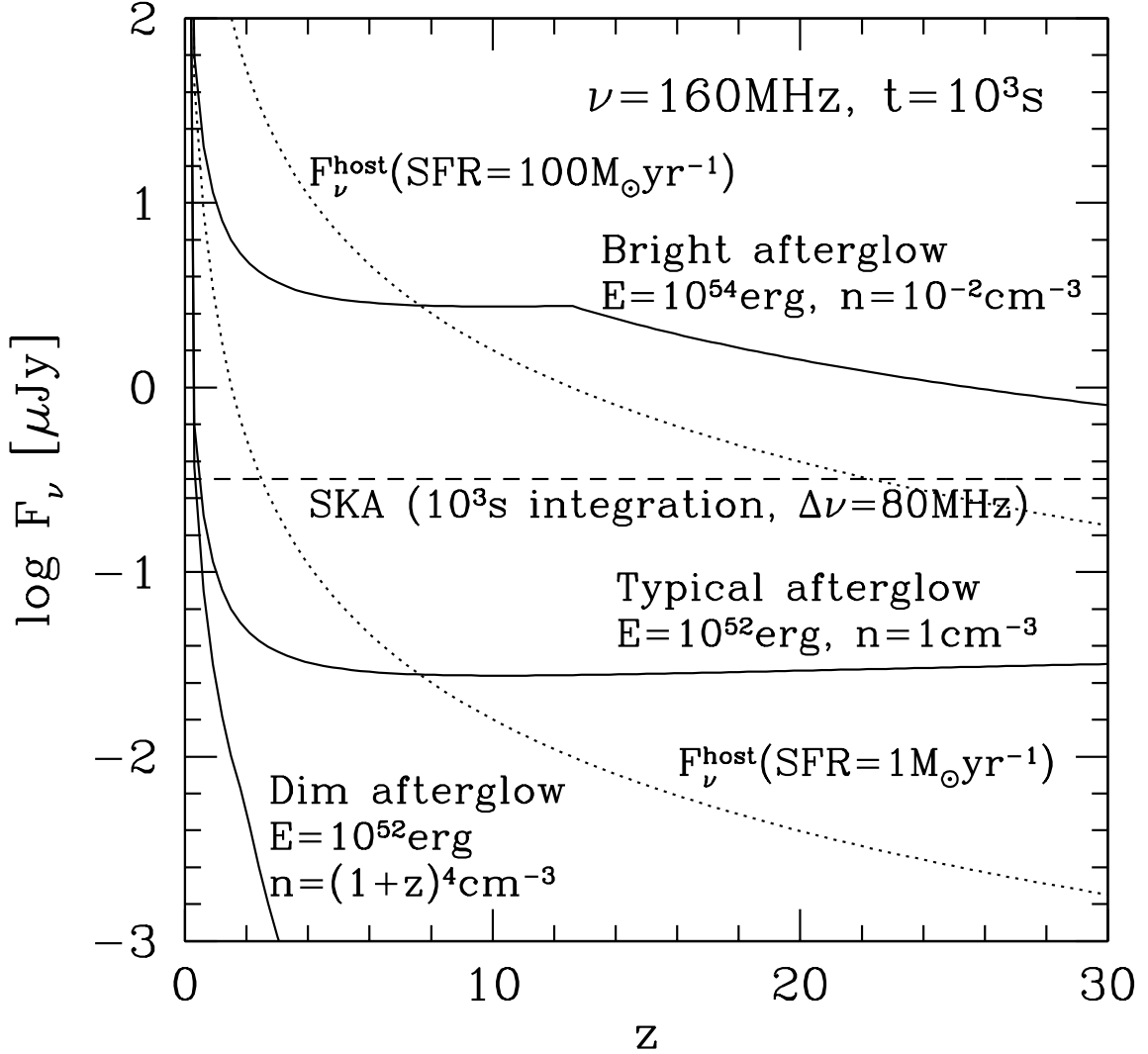


Fig. 3.— The afterglow flux at a frequency $\nu = 160$ MHz and an observer time $t = 10^3$ s is shown as a function of redshift z by the solid lines. We adopt $\epsilon_e = 0.1$, $\epsilon_B = 0.01$ and $p = 2.2$ with $E = 10^{52}$, 10^{54} , 10^{52} erg and $n = 1$, 10^{-2} , $(1+z)^4$ cm^{-3} for typical, bright, dim afterglows, respectively. The rms sensitivity of the Square Kilometer Array for an integration time 10^3 s and a band width $\Delta\nu \sim 0.5\nu$ is plotted by the dashed line. The expected flux of the host galaxy $F_\nu^{\text{host}} \sim 25 [(1+z)\nu/1 \text{ GHz}]^{-0.75} (\text{SFR}/1 M_\odot \text{ yr}^{-1}) (D/1 \text{ Mpc})^{-2} (1+z)$ Jy is shown by the dotted lines where SFR is the star formation rate (Yun & Carilli 2002). At high z , CMB photons may make the host galaxy dimmer by the inverse Compton cooling (Oh 2001).